INTERNATIONAL JOURNAL FOR NUMERICAL METHODS IN FLUIDS
Int. J. Numer. Meth. Fluids 2009; **61**:220–236
Published online 4 November 2008 in Wiley InterScience (www.interscience.wiley.com). DOI: 10.1002/fld.1951

Flow analysis for a double suction centrifugal machine in the pump and turbine operation modes

José González*,†, Jesús Manuel Fernández Oro, Katia M. Argüelles-Díaz and Carlos Santolaria

Universidad de Oviedo, Área de Mecánica de Fluidos. Campus de Viesques, 33271 Gijón (Asturias), Spain

SUMMARY

A double suction centrifugal machine has been studied, both experimentally and numerically, operating as a pump and as a turbine. Experimentally, the static performance of the machine working as a pump was obtained. These measurements were compared with equivalent numerical results from a URANS calculation. As a second step, the numerical results have been exploited to get detailed information about the flow in both operating modes (pump and turbine).

The main goals of the study are, first, the validation of the numerical procedure proposed and second, the possible turbine operation of the impeller, which could point out a wider working range for the machine. The first aspect is handled by detailed analysis in the pump mode, according to previous experience of the research group. The second objective is obtained by using the numerical model to explore the flow fields obtained, when working in an inverse mode. Therefore, the presented results join the use of a numerical methodology and the turbine mode of operation for a centrifugal impeller, providing insight into the flow characteristics.

When working as a pump, the flow at the suction side is characterized by the existence of an inlet tongue, which tends to enforce a uniform flow for the nominal conditions. For the turbine mode, flow patterns in the impeller, volute and suction regions are carefully investigated. The influence of the specific geometrical arrangement is also considered for this operation mode. Copyright © 2008 John Wiley & Sons, Ltd.

Received 22 October 2007; Revised 18 September 2008; Accepted 18 September 2008

KEY WORDS: flow in turbomachines; centrifugal pumps; double suction machine; incompressible flow; experimental data; CFD technique; sliding mesh

*Correspondence to: José González, Universidad de Oviedo, Área de Mecánica de Fluidos. Campus de Viesques, 33271 Gijón (Asturias), Spain.
†E-mail: aviados@uniovi.es

Contract/grant sponsor: Ministerio de Ciencia e Innovación (Spain); contract/grant numbers: DPI2006-15720, DPI-2006-15638-C02-01, TRA2007-62708

INTRODUCTION

The global complexity of any study of the flow in a centrifugal impeller has generated the development of many studies (among others, Karassik *et al.* [1], Neumann [2]). When the geometry of the volute casing has any significant geometrical characteristics, like a double suction at the inlet or a double volute tongue at the outlet, the flow structure becomes even more complex and is still far from being fully understood [2].

The flow in any hydraulic turbomachine is always 3D and unsteady. Therefore, any analysis should be done keeping both the dynamic and 3D effects. Actually, the combination of both gives rise to the real working flow patterns [2]. Although, even today, the design of any of those machines starts with a steady flow assumption, this approach is only valid for operating points near the design or nominal one. Therefore, more complex and accurate data are needed.

The considered geometry in the present study, a double suction pump, is a quite common solution when cavitation problems are likely to arise [3]. They are usually suitable in applications where a high flow rate is needed and in situations where the axial forces could establish a limitation for a conventional model. The main drawback might be the possible increase in the radial forces or the break of the axial balance when increasing the flow rate. As in any pump, the fluid flow is inherently unsteady, and is the most important source of vibration and hydraulic noise [4].

Different numerical methods to treat the URANS equations for turbomachinery applications have been widely developed. This particular field is just an example of the many applications where the numerical solution of the flow has proven its worth [5]. Although predictions of the flow field are always valuable, the numerical simulation of a commercial pump is not easy due to the usual computational fluid dynamics (CFD) difficulties: turbulence modelling, flow separation, boundary layer, etc. [6]. For the case studied here, there are also some particular problems like the extremely difficult geometry (especially at the inlet) and the complex flow dynamic effects. Some clear examples of numerical solutions applied to the dynamic effects on centrifugal pumps have been reported in different References [7–10].

The experimental facilities and apparatus to perform a detailed and dynamic flow analysis inside any hydraulic machine have become more complex and expensive. It is in this arena where the CFD techniques find their direct application. With the updated numerical techniques almost any geometry can be analysed and meaningful information can be obtained [6]. The numerical research on hydraulic machinery has been increasingly used as a design tool, particularly in the field of centrifugal machines [10].

In this paper, a numerical model for the analysis of the flow inside a double suction machine is presented, and the pressure and velocity fields at different locations are analysed. These numerical simulations, performed for different operating conditions and for the two modes of operation (pump and turbine), were carefully analysed and valuable conclusions with regard to the flow structure are reported.

The use of pump impellers as turbines is not new and many efforts have been directed towards the application of such arrangements [11]. From the beginning of such applications until the modern pump–turbines (so widely designed), many improvements and cost effectiveness studies have been carried out. Mainly used for small power, many authors have pointed out the advantages of centrifugal impellers working as turbines (Fernández *et al.* [12], among others). Nevertheless, the use of a double suction geometry to work in the turbine mode could be seen as a source of problems, due to the specific arrangement of this kind of design. Therefore, a need for a better understanding of the flow behaviour inside a double suction machine working in the turbine mode

DOI: 10.1002/fld

is needed. The combination of both a double suction geometry and a numerical study has been the subject of some recent work [3, 10]. In this paper, research into the possible application of a double suction pump working as a turbine is presented.

Once the model was validated through performance curve comparison, the flow patterns in the impeller, volute and suction regions were investigated. The suction flow field is of special interest due to the induced modification of the axial and circumferential velocity fields. In addition, the pressure evolution is considered in order to study the different patterns at the inlet of the pump, where cavitation is likely to arise.

In general, the CFD techniques provide a good approach for predicting general trends in possible new designs or extending them to different operation modes in existing machines. This latter being the point considered in the present study, where a possible working range is explored for the existing pump when operating as a turbine, with optimum efficiency levels. From this study, an optimization of the geometry could also be performed, although this would depend on future requirements and perspectives.

MACHINE DESCRIPTION AND EXPERIMENTAL TESTS

A six blade double aspirating impeller (Figure 1), with a maximum diameter of 0.46 m and a blade angle of 32° at that position, is considered for the study. The volute casing (Figure 2) and pipes present a typical configuration for this kind of machine (see González *et al.* [13]). A vaneless configuration is available, although an inlet tongue is manufactured. This inlet tongue, designed for the pumping mode, becomes an outlet obstacle when working as a turbine.

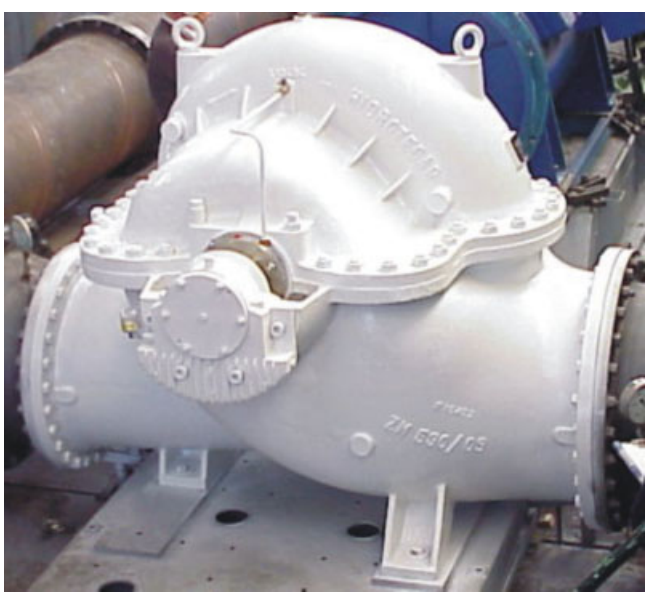

Figure 1. Experimental set-up for the pump measurements (dimensions in m).

DOI: 10.1002/fld

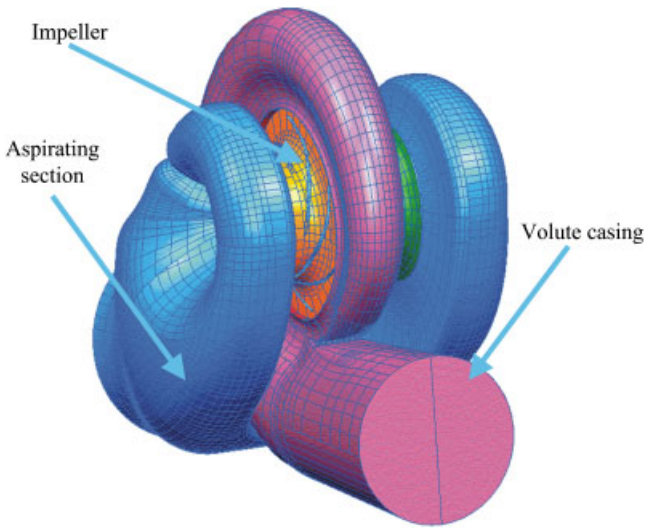

Figure 2. Sketch of the pump unstructured mesh. (Inlet and outlet pipe far enough to impose boundary conditions.)

Table I. Machine main dimensions and nominal operating points.

Number of blades	$z=6$
Impeller outlet diameter	$D_2=0.46\,\mathrm{m}$
Outlet blade angle	$\beta_2=32^\circ$
Rotational speed	$\omega=\pm154.99\,\mathrm{rad/s}$
Nominal flow rate (pump mode)	$Q_\mathrm{N}=0.694\,\mathrm{m}^3/\mathrm{s}$
Head at nominal flow rate (pump mode)	$H_\mathrm{N}=49.50\,\mathrm{m}$
Specific speed (pump mode)	$\omega_\mathrm{s}=1.25$
Nominal flow rate (turbine mode)	$Q_\mathrm{N}=0.708\,\mathrm{m}^3/\mathrm{s}$
Head at nominal flow rate (turbine mode)	$H_\mathrm{N}=59.80\,\mathrm{m}$
Specific speed (turbine mode)	$\omega_\mathrm{s}=1.13$

In the hydraulic set-up used for the experiments, water was pumped from and returned to a $200\,\mathrm{m}^3$ reservoir. The tested pump had a single double suction duct and a vaneless spiral volute casing. The main parameters of this pump are presented in Table I. The rotational speed was set to $\omega=\pm154.99\,\mathrm{rad/s}$, which is a positive value for the pump mode and negative for the turbine one.

Standard pressure manometers were used for the head measurements. To obtain the flow rate, an electromagnetic Krohne flow-meter was installed. Flow rate uncertainties were found to be always less than $\pm2.5\%$ (confidence level of 95%). The head and efficiency uncertainties were kept under $\pm1.5\%$ for the pump mode, within the same confidence level. All uncertainty analyses were carried out following the procedures proposed in Kline [14].

No experimental results were available for the turbine operation mode. For this operating mode, the goal of the study was to find the machine possibilities to work in an efficient and reliable way.

The relative high specific speed and the double suction at the inlet are the relevant features of the studied pump. A definition of the flow features can be obtained if the numerical model is

DOI: 10.1002/fld

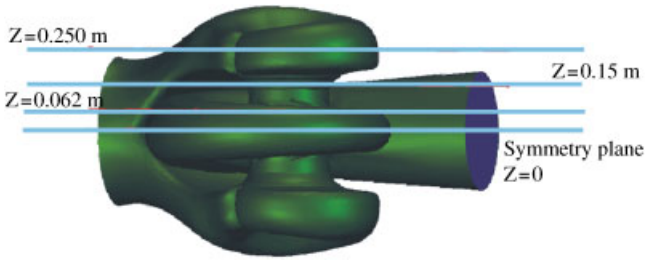

Figure 3. Sketch of the pump defining the reference planes.

considered (Figure 3). The reference planes shown in this Figure 3 will be used in the following stages of the study. The symmetry plane ($Z=0$) sets the reference for different planes in which the increasing Z (values higher than $Z=0.15$) means a section placed more upstream of the rotor inlet.

NUMERICAL MODEL

The 3D unsteady Navier–Stokes equations were solved using the FLUENT software. Owing to symmetry considerations, only half of the pump was modelled.

Geometry and grid

The discretization of the geometry was done keeping the balance between calculation time (details are included in the section on numerical solution control) and the accuracy of the simulation for the flow structure. In any case, the average CPU time was kept on the order of 350 h. Special care was observed in the region near the tongue by carrying out a detailed study of flow vectors and stagnation point placement. An unstructured mesh of tetrahedral cells was generated to define the inlet and outlet zones (more than 100 000 cells and around 150 000 cells, respectively) and the same kind of cells were used to define the impeller and volute (almost 250 000 cells and 235 000 cells, respectively). In the volute, a mesh-refined zone was defined for the region close to the tongue. The particular features of the mesh were also compared with previous experience of the group (for example, see González *et al.* [10]) and found to be appropriate. Some global tests (with the whole machine) also indicated that cell number was in the required range.

Once the geometry was defined, the model was ready to be used in the numerical simulations. The final grid generated for the inlet section, the volute and the impeller are shown in Figure 4. The sliding mesh technique has been widely used in the last decades by turbomachinery researchers (for instance, for a centrifugal pump application, see Croba and Kueny [9]). It basically consists of a numerical procedure that allows a proper variable transfer from a moving mesh onto a static one. Therefore, it becomes very straightforward to use in a turbomachine, where the impeller rotates and there are also static parts. Obviously, this features need to be considerer here. Two different meshes are considered, one rotating with the impeller while the other remains static (inlet and outlet pipes and the two volutes). Consequently, two sliding zones must be defined to allow the relative motion of the meshes in both inlet and outlet sections.

DOI: 10.1002/fld

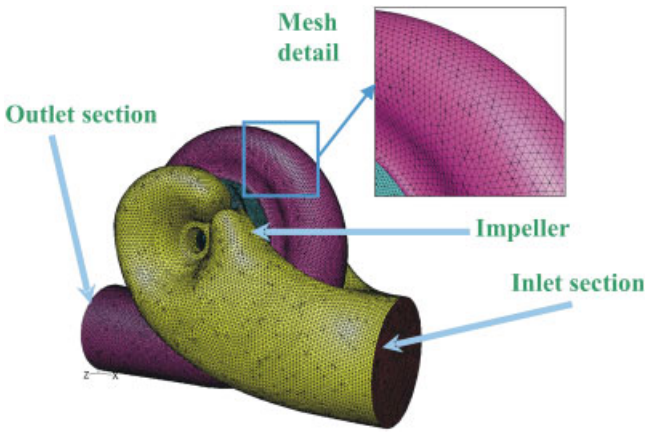

Figure 4. Unstructured mesh considered for the numerical study (a detail is enlarged).

Mathematical model

The numerical code used (FLUENT) solves the fully 3D incompressible Navier–Stokes equations, including the centrifugal force source in the impeller and the unsteady terms. Turbulence was simulated with the standard k–ε model. Although grid size was not adequate to investigate the local boundary layer variables, global values were well captured and the details of the flow near the tongue seems to follow the usual trends found in the bibliography [4]. Wall functions based on the logarithmic law were used for the flow calculations. The time-dependent term was discretized with a second-order implicit scheme. The pressure–velocity coupling was calculated through the SIMPLEC algorithm. Second-order, upwind discretizations were used for convection terms, and central difference schemes for diffusion terms. This procedure has been widely used with big success for other geometries [10].

Boundary conditions

The modelled boundary conditions were the ones considered with the most physical meaning for turbomachinery flow simulations. For the pump operating mode, those were total pressure equal to zero at the inlet and a pressure drop proportional to the kinetic energy at the outlet. The flow rate was changed by modifying the constant for that pressure drop at the outlet condition, which simulates the closure of a valve. Again, the no-slip condition with a logarithmic law for the boundary layers was imposed over the impeller blades and walls, the volute casing and the inlet pipe wall. Using this boundary conditions, comparison between different operating points can give rise to possible cavitation inception detection (same pressure level at the inlet), although this is not the goal in this research.

For the turbine operating mode, static pressure was set equal to zero at the exit and a total pressure was imposed at the inlet. The flow rate was changed by modifying the total pressure at the inlet. Again, the no-slip condition with a logarithmic law for the boundary layers was imposed over the impeller blades and walls, the volute casing and the inlet pipe wall. Using these boundary conditions, comparison between different operating conditions was straightforward.

DOI: 10.1002/fld

The boundary conditions for the turbulence model are fixed at the inlet of each domain, which change depending on the operation mode. The k–ε closure model works with the input of the inlet turbulence level, in percentage of the inlet velocity. From that, it obtains the kinetic turbulence energy (k), and with the inlet diameter it internally calculates the derived turbulent variables (ε and the eddy viscosity).

Numerical solution control

A cluster with 20 Athlon-K7 nodes was used for the calculations. The time step used in the unsteady calculation was set to 0.0002703 s in order to get enough time resolution for the dynamic analysis (the Courant number was kept below 3, which assures very good time accuracy and numerical stability). Mesh independency was studied only through local refinement near the volute tongue. Some preliminary test with lower number of cells indicated neither local nor global flow variations. This approach is selected due to the obvious numerical restriction in terms of CPU time. Although it can be observed as a weakness of the model, the bigger cell size is in the range considered as optimum for other centrifugal pump geometries, previously studied by the authors [10, 15].

The number of iterations was adjusted to reduce the residual below an acceptable value in each time step. In particular, the ratio between the sum of the residuals and the sum of the fluxes for a given variable in all the cells was reduced to the value of 10^{-5} (five orders of magnitude). Initializing the unsteady calculation with the steady solution, over 10 impeller revolutions were needed to achieve the periodic unsteady solution convergence. Such calculations correspond to an average CPU time of 350 h.

The numerical accuracy of both steady results (either for the pump or turbine operation modes) was estimated to be on the order of 2 and 1.5%, respectively. During the numerical study, the guidelines proposed in [16] were used and the numerical uncertainty was related to the change in certain reference values when different mesh refinements were considered. Therefore, the values obtained for accuracy can be considered reasonable enough as to validate the numerical results.

STATIC RESULTS AND DISCUSSION FOR BOTH OPERATION MODES

After the periodic state was obtained, the unsteady results were averaged over a blade passing interval. The first comparison is made for the performance curves working as a pump and is shown in Figure 5. For these performance curves, the axes are made non-dimensional using the relationships:

$$\phi = \frac{Q}{\pi D_2 b_2 U_2} \tag{1}$$

$$\psi = \frac{gH}{U_2^2/2} \tag{2}$$

where the subscript 2 refers to the outlet section for the pump mode, and to the inlet when the machine is working as a turbine. As can be observed for the head curve, the prediction of separation at low flow rates is not fully accomplished with the numerical solution and some differences are found at the lower flow rates. However, at nominal and higher flow rates, both the numerical and the experimental curve are almost one on top of the other. For the general comparison, the agreement found between both curves has encouraged the research; hence, detailed flow analysis has been performed and will be explained in what follows.

DOI: 10.1002/fld

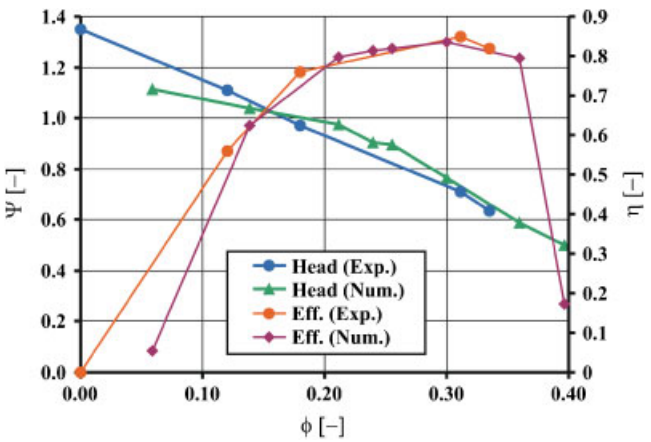

Figure 5. Comparison of the performance curves (non-dimensional variables).

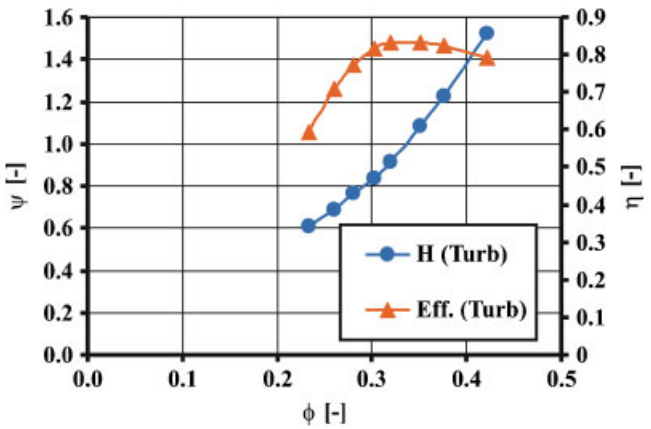

Figure 6. Performance curves for the turbine mode of operation (numerical prediction).

Nominal flow rate is numerically predicted at $\phi = 0.30$, slightly lower than the experimentally predicted one ($\phi = 0.32$). Therefore, the agreement for the determination of this nominal flow rate is considered very good.

For the efficiency curves, more differences are found. An explanation for such differences comes from the fact that the torque for the experimental efficiency calculation was measured in the shaft, while the numerical torque does not consider the mechanical losses and the disk friction at the impeller hub and shroud.

Considering the turbine mode, no comparison with experimental results is possible, and the numerical study of the same impeller geometry was carried out to analyse the possibilities of such a geometry working as a turbine. With the proposed boundary conditions, a full evolution of the performance curve was obtained. For such purposes, torque and required head as a function of the

DOI: 10.1002/fld

flow rate are plotted in Figure 6. These performance curves were obtained for the same rotational speed as the pump, but with opposite direction, that is, $\omega = -154.99\,\mathrm{rad/s}$.

As can be seen in Figure 6, typical behaviour of the impeller working as a turbine can be seen in the performance curves. In particular, an almost constant efficiency of 80% for flow rates varying in the range $\phi = 0.3$–0.4, followed by a quick fall for lower flow rates, was predicted numerically. The required total head at the inlet also follows typical turbine trends.

The shape of the curves agrees with the expected trend for a centrifugal turbine [11]. The best efficiency point flow rate is relatively similar to the equivalent one for the pump mode. Accepting these numerical results, a detailed flow analysis was also carried out for the turbine mode, with the aim of finding the most relevant flow occurrences if the operation of the machine as a turbine was to be put into practise.

DETAILED FLOW ANALYSIS FOR THE PUMP MODE

The averaged unsteady fields were obtained for different flow rates in order to analyse the different working conditions inside the pump. With this goal in mind, the pressure and velocity for different positions of the impeller were obtained numerically. An example of the static pressure values for the symmetry plane is shown in Figure 7. In this case, the nominal flow rate is considered and therefore, a quite axi-symmetric pattern for the pressure distribution in the impeller is obtained.

From now on, the blade passing average values are presented in order to explain the global behaviour and the model feasibility to describe the particular flow features. Previous studies for a single suction centrifugal pump [17] have pointed out the relevancy of the detailed flow analysis, as will be performed in the following.

The study of the flow conditions at different sections is first focused on the calculated structure around the volute. For a low flow rate (see Figure 8 for $\phi = 0.13$), an important acceleration region together with an important low-speed region is observed near the tongue. The separation point is placed somewhere downstream of the volute tongue in the discharge direction, which agrees with the expected trend for a centrifugal pump (see Miner *et al.* [18]).

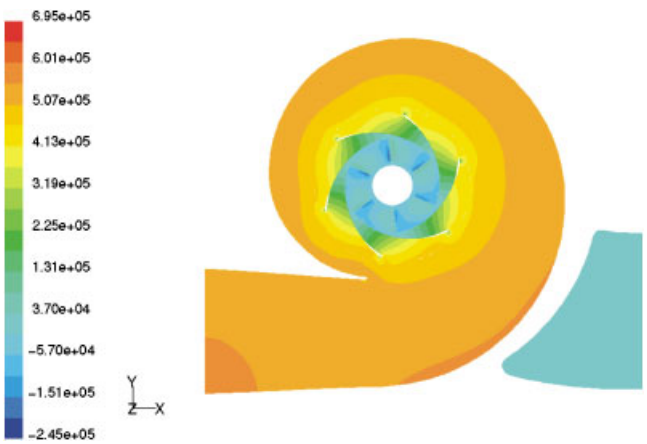

Figure 7. Static pressure distribution in the $Z = 0$ plane for the nominal flow rate ($\phi = 0.30$).

DOI: 10.1002/fld

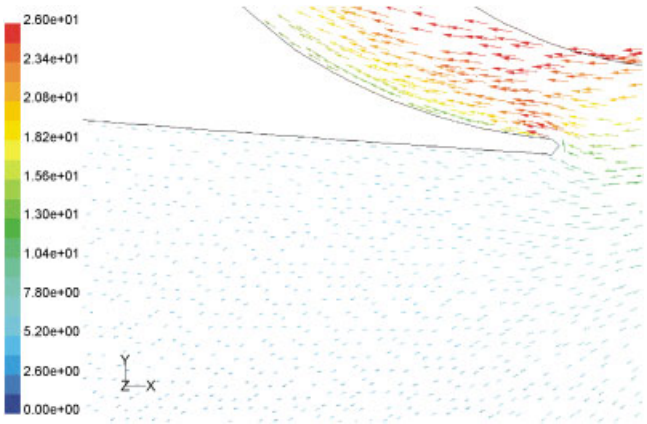

Figure 8. Velocity field around the volute tongue for $\phi = 0.13$.

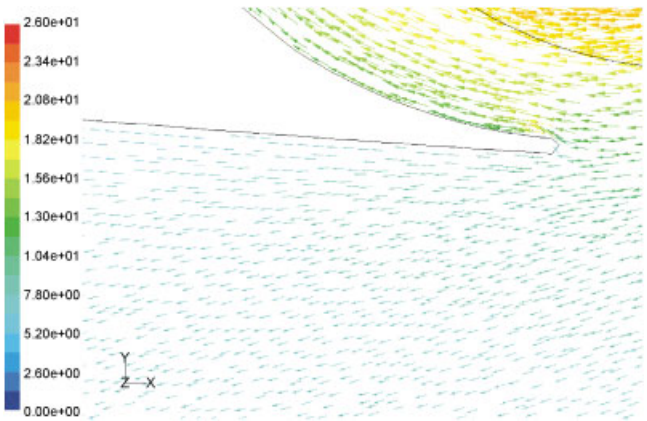

Figure 9. Velocity field around the volute tongue for $\phi = 0.30$.

For the nominal flow rate (as can be seen in Figure 9), a better flow distribution around the tongue was obtained. Therefore, a minimum loss condition is attained for flow rates close to the one in this figure, $\phi = 0.30$. At this operating point, the tongue softly divides the flow into two parts.

For flow rates higher than the nominal one (Figure 10 for $\phi = 0.36$), a strong re-circulation bubble is found downstream of the tongue in the volute direction. Again, the losses are increased and the relative position of the separation point agrees with the expected trend for low flow rates.

The effect of the inlet geometry is considered next. For this purpose, pressure at two sections is averaged and presented here. The two sections are $Z = 0.250\,\text{m}$ (side inlet of the pump) and $Z = 0.15\,\text{m}$ (just before the impeller). For both sections and three different flow rates (nominal one, low and high) the pressure is considered. The same colour scale is maintained to allow a direct comparison of the results.

DOI: 10.1002/fld

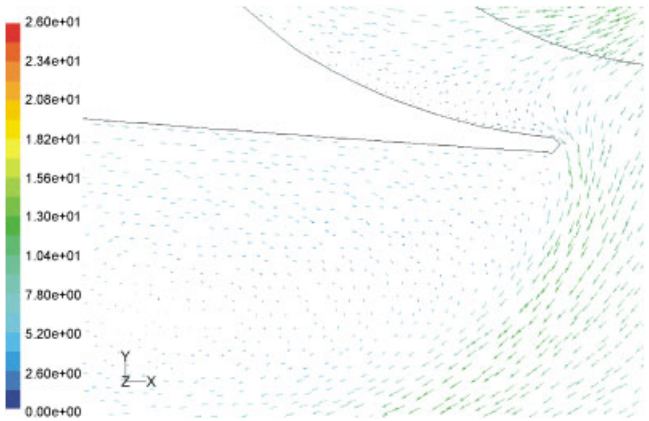

Figure 10. Velocity field around the volute tongue for $\phi = 0.36$.

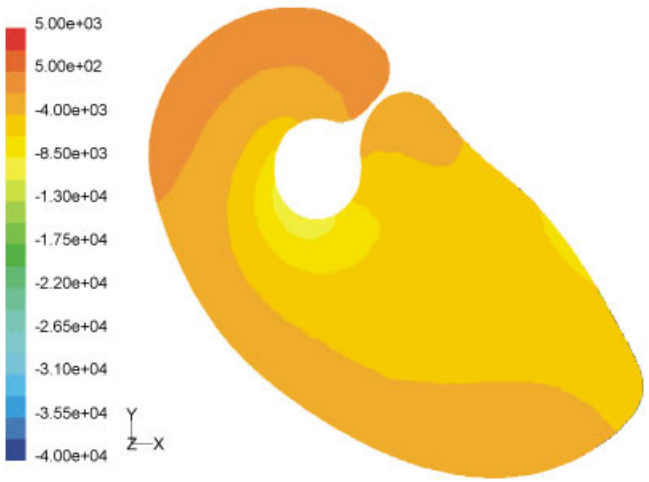

Figure 11. Static pressure distribution at the semi-volute suction inlet ($\phi = 0.13$).

In the first section ($Z = 0.250$ m), the geometry of the pump introduces a semi-volute at the inlet suction, aiming at uniform flow conditions (at least for nominal flow rates, Neumann [2]). The effect of this second geometrical constraint is superimposed on the tongue effect (in the discharge volute) and shortens the range of flow rate that has reasonably good efficiency (Figure 5).

Three different flow rates are analysed using a 45 000 Pa scale (from −40 000 to 5000 Pa) for the averaged pressure field, and the numerical results are shown in Figures 11–13. The total pressure at the inlet is always set to zero. The flow in the pump mode evolves in a direction normal to the drawing plane and then around the central orifice. In the case of a good inlet duct design, this would impose a uniform inlet condition. Figure 12 shows the pressure field for the nominal flow rate and as can be observed, a quite uniform inlet condition is produced. For the other figures

DOI: 10.1002/fld

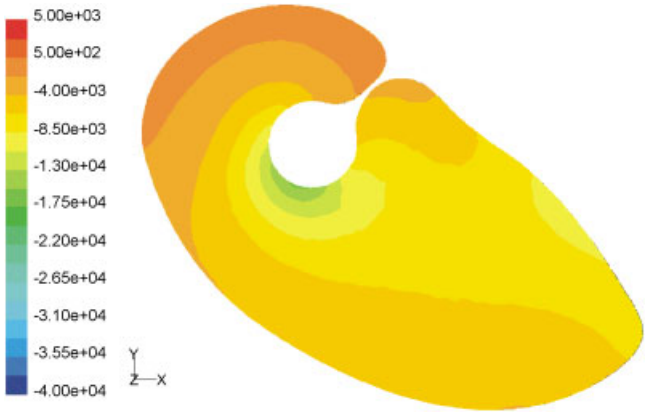

Figure 12. Static pressure distribution at the semi-volute suction inlet ($\phi = 0.30$).

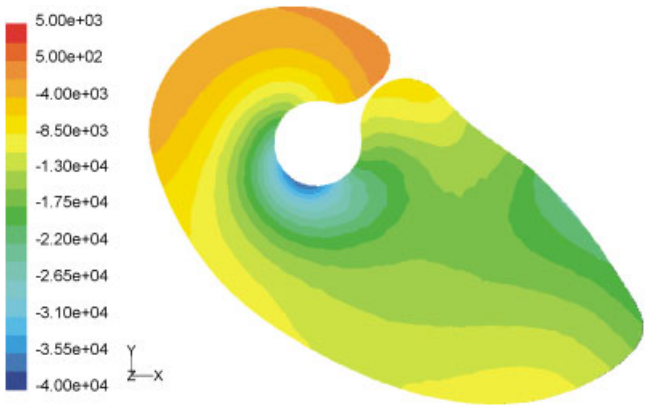

Figure 13. Static pressure distribution at the semi-volute suction inlet ($\phi = 0.36$).

showing the pressure distributions (Figures 11 and 13), the pressure patterns look similar, although the pressure changes are larger in Figure 13 due to the higher velocity.

No reverse flow from the impeller is observed when the velocity fields are analysed, even at low flow rate ($\phi = 0.13$). Nevertheless, the effect of the flow deceleration on the concave hub side at the inlet is found and plotted in a plane normal to the Z-axis (see Figure 14).

Considering these pressure distribution figures, the conclusion to be drawn is that the semi-volute at the suction inlet works quite well in producing a uniform inlet for nominal flow rate. The numerical results point out a better uniformity for low flow rates in the sections upstream of the impeller, but when approaching the impeller, the uniform inlet is obtained for flow rates close to the nominal one.

Some possible cavitation problems are likely to be found. Static pressure of $-100\,000$ Pa, relative to the 0 Pa imposed as total pressure at the domain inlet, was found for the highest flow rate in a very narrow zone at the impeller inlet. The effect of this possible problem should be taken into

DOI: 10.1002/fld

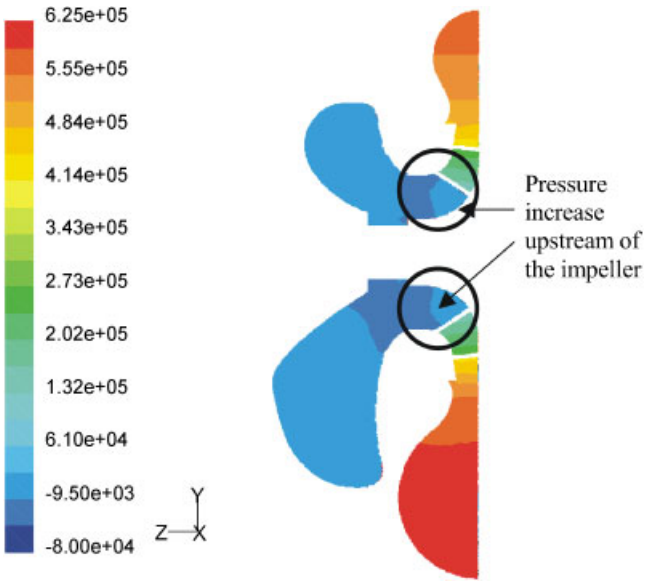

Figure 14. Static pressure field at the $X=0$ plane, $\phi=0.13$.

account as far as the operation of the studied machine, and would be of interest for such flow rates. However, this is not the main goal of the present paper.

As previously mentioned, the dynamic effects (studied in Parrondo *et al.* [17] for a simple aspiration centrifugal pump) have not been analysed in this paper, due to the lack of experimental measurements with which to compare. However, the unsteady model developed here can be focused on this direction in the near future.

DETAILED FLOW ANALYSIS FOR THE TURBINE MODE

Owing to the unsteady procedure used during the calculation, an averaging method had to be introduced in order to analyse the flow field. The average passage flow was considered for three flow rates. To cover the maximum range, these three flow rates correspond to the nominal one (maximum efficiency in Figure 7), and the maximum and minimum simulated flow rates. Two different sets of figures are discussed here, containing the averaged pressure and velocity values for a blade passing period. Two different sections of the flow region have been considered and will be shown. First, the semi-volute section (same section as shown in Figures 11–13) is presented and then, a flow analysis in the impeller is described.

In Figure 15, the absolute velocity field at the exit casing with the presence of the semi-volute tongue is plotted for three different flow rates. In particular, $\phi=0.23$ or low flow rate is plotted in the upper left side of the figure, $\phi=0.32$ or nominal flow rate is plotted in the upper right side, and $\phi=0.42$ or high flow rate is plotted in the lower part of the figure. The same velocity scale is considered for the three figures (0–11 m/s), and they are grouped to better understand

DOI: 10.1002/fld

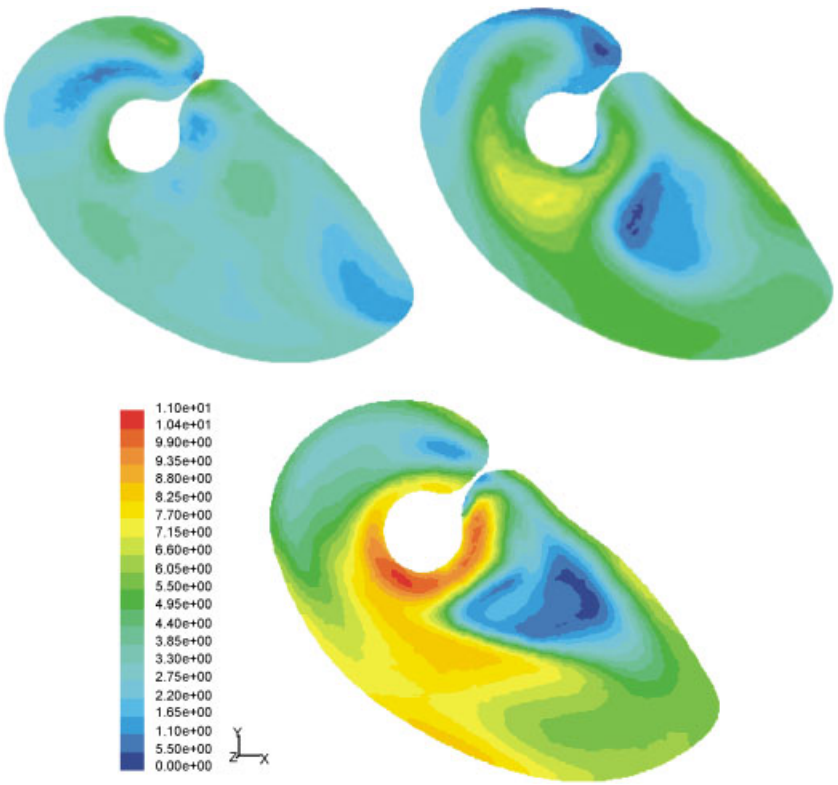

Figure 15. Averaged velocity fields at the exit section. Velocity magnitude is plotted for $\phi = 0.23$ (upper left map), $\phi = 0.32$ (upper right map) and $\phi = 0.42$ (lower map).

the comparisons. As stated before, the semi-volute tongue is introduced to produce uniform flow conditions. These conditions are not as important in the turbine mode of operation as the semi-volute tongue is now at the flow outlet.

Nevertheless, and for the nominal and lower flow rates, quite uniform velocity contours are clearly obtained. One must consider that for such a range of low flow rates, lower velocities are found and the velocity gradients become less important. At higher flow rates (lower part of the Figure 15), the velocity range increases. Somehow, the outlet condition is still uniform, as observed in the near impeller exit zone. Obviously, the velocity there has also increased in comparison with the previously analysed flows, but the average value at that exit zone is kept reasonably constant. However, in contrast to the lower flow rates, a large area with a strong velocity gradient is found downstream. This is visible at the right side of the high flow rate figure: a region with almost zero velocity is very near to the region with a velocity around 7.0 m/s. As a straightforward effect, lack of axial symmetry is produced and more losses are created. The use of the machine at this flow rates should be limited to short operation times, but never considered as a permanent working condition. Other zones with different flow distributions are found in the upper part of the figures. A minimum of velocity is observed for the nominal flow rate in the zone. Therefore, a minimum in the post-rotation of the flow is produced downstream for this nominal condition.

DOI: 10.1002/fld

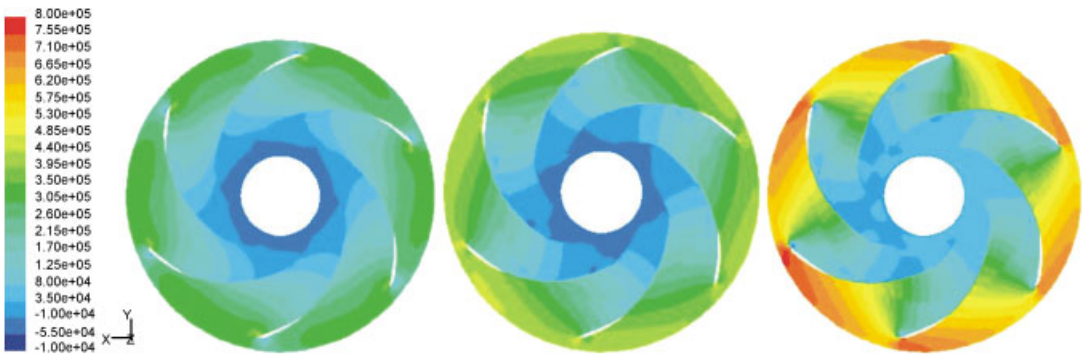

Figure 16. Averaged pressure fields in the turbine. $\phi = 0.23$ (left-hand side), $\phi = 0.32$ (centre) and $\phi = 0.42$ (right-hand side).

The averaged pressure field in the impeller is plotted in Figure 16. The same three flow rates considered in Figure 15 are now studied, but for the relative flow conditions. Again, a standard pressure range is considered to allow ease of comparison. In particular, a range from $-100\,000$ to $+800\,000$ Pa scale is used for the three flow rates. The three fields correspond to $\phi = 0.23$, at the left side of the figure, $\phi = 0.32$ or nominal flow rate, plotted in the centre of the figure, and finally $\phi = 0.42$, placed at the right-hand side of the figure. The area plotted in this figure corresponds to the hub of the turbine from the inlet (without the casing) and the curved surface is, therefore, observed as the inlet circle (without the outlet section, in the middle).

Very constant pressure field is recovered for the nominal flow rate (centre of the figure) for a given radial position (any circle considered in the figure). That is, a very uniform pressure decrease is found from inlet to outlet of the impeller.

For both low and high flow rates (placed, respectively, at the left- and right-hand side of the figure), stronger effect of the blades is observed. Note that for the higher flow rate (right-hand side figure), a quite important lack of axial symmetry is found. As expected, the possible cavitation effects are higher at low flow rates. For such operation conditions (as can be observed in the left-hand side figure) there is also a possible cavitation zone at the blades inlet section.

A stronger flow periodicity can be observed (softer and more periodic pressure decrease from the inlet to the outlet section) if one compares the central figure with the ones at its sides. In addition, considering the previously shown velocity field, a smaller change in the flow direction is recovered relatively to the blade angle for the nominal flow rate.

Figures 15 and 16 show the maximum and minimum flow rates studied for the turbine operation mode. There have also been some intermediate flow rates analysed numerically, but these flow rates do no present any contradictory results and, therefore, conclusions have been grouped into low, nominal and high flow rates. Higher or lower flow rates, in comparison with the ones studied, would be of no practical interest for the considered geometry.

The observed flow patterns for the turbine mode of operation stress the fact that the proposed geometry would perform quite well for the nominal and lower flow rates. The modelled fields do point to poor operation for high flow rates. If this machine would be installed in a reversing operation hydraulic plant, the observed limitations would not be a problem, as for such applications a high flow rate operating regime is only required for the pumping mode. Considering the performance

DOI: 10.1002/fld

curves (Figure 6) together with the local flow analysis carried out, the geometry shows a good behaviour for a wide range of working conditions.

CONCLUSIONS

An analysis of the flow inside a double aspirating centrifugal machine has been carried out. The study is performed using a CFD technique based on the sliding mesh and the real movement of the impeller. Comparisons with experimental data are available for the pump operation mode.

For the pump mode, design and off-design values have been recorded and a very good agreement has been found for the performance curve measured experimentally. The separation zones in the vicinity of the volute tongue have been observed in the numerical model and do agree with the expected trends, according to the bibliography.

One particular feature found for the studied pump mode is the lack of a uniform inlet condition, except for flow rates near the nominal one. It seems that the pump geometry produces a deviation from the axi-symmetric flow distributions even for small differences (above and below) from the nominal flow rates. This might lead to important radial forces that could limit the use of this particular design.

In spite of the difficulties induced by the geometrical complexity at the exit of the machine when working as a turbine (due to the double arrangement with a flow splitting effect), relative high efficiencies were predicted for the impeller under consideration (values up to 80%). As in any turbine, the regulation and piping systems should be carefully designed to avoid possible unsteady phenomena.

Working as a turbine, and from the detailed flow analysis, a confirmation of the general and global trends observed on the performance curve were made possible. The higher flow rate studied gave rise to an important lack of uniform conditions for the flow inside and after the impeller. Therefore, the optimum working range for this impeller in a turbine mode is more limited than expected from the performance curve.

The cost effectiveness and proper working variables have been predicted numerically for the studied geometry. Some complementary experimental results for the turbine mode of operation and for the dynamic flow structure would be of interest if a full validation of the numerical data obtained was to be considered. Despite this lack of experimental data, the numerical results do improve the knowledge of the flow features inside a complex machine and, basically, point out to a good performance in both operation modes.

NOMENCLATURE

D_2	impeller diameter at outlet (m)
H, H_N	pump head and pump head at the best efficiency point (nominal) (m)
k	turbulent kinetic energy (m^2/s^2)
Q, Q_N	flow rate and flow rate at nominal point (m^3/s)
t	time (s)
U_2	peripheral velocity at impeller outlet (m/s)
X, Y, Z	coordinate system (m)
z	number of blades (dimensionless)

DOI: 10.1002/fld

β_2	impeller blade angle (outlet section) (deg.)
ε	turbulent dissipation (m^2/s^3)
ϕ	flow coefficient, see Equation (1) (dimensionless)
ρ	density of the fluid (water in this paper) (kg/m^3)
ω, ω_s	rotating speed and specific speed, respectively, where $\omega_s = \omega Q_N^{1/2}/(gH_N)^{3/4}$ (rad/s) and (dimensionless)
ψ	head coefficient according to Equation (2) (dimensionless)
η	machine efficiency (dimensionless)

ACKNOWLEDGEMENTS

The authors acknowledge the financial support from the 'Ministerio de Ciencia e Innovación' (Spain), under projects DPI2006-15720, DPI-2006-15638-C02-01 and TRA2007-62708.

REFERENCES

1. Karassik IG, Krutzsch WC, Fraser WH, Messina JP. *Pump Handbook* (2nd edn). McGraw-Hill: New York, 1985.
2. Neumann B. *The Interaction Between Geometry and Performance of a Centrifugal Pump*. MEP: London, 1991.
3. Kyung C, Pyun P, Hyun C, Sang L. A study of flow analysis for a double suction centrifugal pump. *Proceedings of the Fluids Engineering Division Summer Meeting*, *FEDSM2002-31180*, Montreal, Canada, 2002.
4. Brennen CE. *Hydrodynamics of Pumps*. Oxford University Press and CETI Inc: Oxford, 1994.
5. Gunzburger MD, Nicolaides RA. *Incompressible Computational Fluid Dynamics. Trends and Advances*. Cambridge University Press: Cambridge, 1993.
6. Laskminarayana B. *Dynamics and Heat Transfer of Turbomachinery*. Wiley/Interscience: New York, 1996.
7. Shi F, Tsukamoto H. Numerical study of pressure fluctuations caused by impeller-diffuser interaction in a diffuser pump stage. *Journal of Fluids Engineering* 2001; **123**:466–474.
8. Tsukamoto H, Uno M, Hamafuku N, Okamura T. Pressure fluctuation downstream of a diffuser pump impeller. *ASME FED* (*Unsteady flows*) 1995; **216**:133–138.
9. Croba D, Kueny JL. Numerical calculation of 2D, unsteady flow in centrifugal pumps: impeller and volute interaction. *International Journal for Numerical Methods in Fluids* 1996; **22**:467–481.
10. González J, Fernández J, Blanco E, Santolaria C. Numerical simulation of the dynamic effects due to impeller-volute interaction in a centrifugal pump. *Journal of Fluids Engineering* 2002; **124**:348–355. DOI: 10.1115/1.2173294.
11. Kittredge CP. Centrifugal pumps used as hydraulic turbines. *Transactions of the ASME Journal of Engineering for Power* 1961; **83**:74–78.
12. Fernández J, Santolaria C, Ballesteros R, Blanco E. Test facility of inverse-working pumps for small and very small hydro-power plants. *Proceedings of the International Congress on Hydropower into the Next Century*, Barcelona, Spain, vol. 1, 1995; 657–664.
13. González J, Santolaria C, Castro F, Parra MT. Numerical model for the unsteady flow behaviour inside a double suction pump. *Proceedings of the Fluids Engineering Division Summer Meeting*, *FEDSM2003-45396*, Hawaii, U.S.A., vol. 2B, 2003; 1149–1155.
14. Kline SJ. The purposes of uncertainty analysis. *Journal of Fluids Engineering* 1985; **107**:153–160.
15. González J. Modelización Numérica del Flujo no Estacionario en Bombas Centrífugas. Efectos Dinámicos de la Interacción entre Rodete y Voluta. *Ph.D. Thesis* (in Spanish), Universidad de Oviedo, Spain, 2000.
16. Freitas CJ. Journal of fluids engineering editorial policy statement on the control of numerical accuracy. *Journal of Fluids Engineering* 1993; **115**:339–340.
17. Parrondo JL, González J, Fernández J. The effect of the operating point on the pressure fluctuations at the blade passage frequency in the volute of a centrifugal pump. *Journal of Fluids Engineering* 2002; **124**:401–410. DOI: 10.1115/1.1493814.
18. Miner SM, Flack RD, Allaire PE. Two dimensional flow analysis of a laboratory centrifugal pump. *Journal of Fluids Engineering* 1992; **114**:333–339.